Electronic, magnetic and transport properties of graphene ribbons terminated by nanotubes

2012 New J. Phys. 14 123012

(http://iopscience.iop.org/1367-2630/14/12/123012)

New Journal of Physics
The open access journal for physics

Electronic, magnetic and transport properties of graphene ribbons terminated by nanotubes

M A Akhukov, Shengjun Yuan[1], A Fasolino and M I Katsnelson
Institute for Molecules and Materials, Radboud University of Nijmegen, Heijendaalseweg 135, 6525-AJ Nijmegen, The Netherlands
E-mail: s.yuan@science.ru.nl

New Journal of Physics **14** (2012) 123012 (11pp)
Received 17 September 2012
Published 10 December 2012
Online at http://www.njp.org/
doi:10.1088/1367-2630/14/12/123012

Abstract. We study, by density functional and large-scale tight-binding transport calculations, the electronic structure, magnetism and transport properties of the recently proposed graphene ribbons with edges rolled to form nanotubes. Edges with armchair nanotubes present magnetic moments localized either in the tube or the ribbon and of metallic or half-metallic character, depending on the symmetry of the junction. These properties have potential for spin valve and spin filter devices with advantages over other proposed systems. Edges with zigzag nanotubes are either metallic or semiconducting without affecting the intrinsic mobility of the ribbon. Varying the type and size of the nanotubes and ribbons offers the possibility to tailor the magnetic and transport properties, making these systems very promising for applications.

Contents

1. Introduction 2
2. Edges terminated by armchair nanotubes 2
3. Edges terminated by zigzag nanotubes 9
4. Summary and conclusion 10
Acknowledgments 10
References 10

[1] Author to whom any correspondence should be addressed.

1. Introduction

The atomic structure of graphene edges is important for the determination of the electronic and magnetic properties of graphene, especially for narrow graphene nanoribbons [1–12]. The natural termination of graphene is given either by zigzag (ZZ) or armchair (AC) edges. Theoretical studies [3] found that the minimal energy structure is instead given by a reconstruction of the ZZ edges to form pentagons and heptagon (57) but this structure has been only rarely observed [13, 14], possibly due to a large free energy barrier [15]. A recent theoretical work [16] on the stability of different graphene edge structures has shown that graphene edges can also fold back on themselves and reconstruct as nanotubes, with low formation energy (see the atomic structures in figure 1). Previous theoretical work had considered such a structure among many other possible configurations made by a combination of nanotubes and graphene nanoribbons [17, 18], suggesting that such a structure could be formed in solution.

In this paper, we show that, besides protecting the edges from contamination and reconstructions, nanotubes at the edges may lead to magnetism and are not detrimental for the electronic mobility despite the row of sp^3 hybridized atoms at the ribbon–tube junction. We study the electronic and magnetic properties of these systems by a combination of DFT and large-scale tight-binding (TB) simulations of transport properties. Our calculations suggest that these systems could be used for a variety of applications that we sketch in figure 2.

2. Edges terminated by armchair nanotubes

We consider systems formed by a nanoribbon terminated on both sides by the same AC or ZZ nanotube. We note that a ribbon with AC edges is terminated by ZZ nanotubes and a ribbon with ZZ edges is terminated by AC nanotubes. Nanoribbons terminated by AC nanotubes present interesting magnetic properties. By rolling the ZZ edges of a nanoribbon, two types of AC nanotubes can be formed, as shown in figure 1. If the atoms at the nanoribbon ZZ edge scroll and bind to the same sublattice sites within the nanoribbon, the formed AC nanotube has mirror symmetry with respect to the nanoribbon plane; if the bonding sites belong to opposite sublattice, there is no such kind of symmetry (compare figure 1(b) with (a)). We call these two cases *symmetric* and *asymmetric* which correspond to *armchair* and *armchair-like* in [16], respectively. The common point of these two cases is that the sublattice symmetry is broken, because all the sp^3 hybridized carbon atoms at the junction belong to one sublattice as shown in figure 3. Due to the Lieb theorem [8, 12], this gives the possibility of spin polarization around the junctions. Since the theorem applies to the Hubbard model, accurate calculations for the real system are necessary to investigate this possibility. Besides these symmetry considerations relevant for graphene, a general condition for magnetism that derives from the Stoner criterion is the presence of peaks in the density of states (DOS) at the Fermi energy for non-spin-polarized calculations. As we show in the following, both symmetric and asymmetric ZZ nanoribbons terminated by AC nanotubes present such peaks and therefore are good candidates for magnetism since they satisfy both the Lieb and Stoner requirements.

In order to study the magnetic properties, we performed (spin-polarized) DFT calculations by SIESTA [20–22]. We used generalized gradient approximation with the Perdew–Burke–Ernzerhof parameterization [23] and a standard built-in double-ζ polarized [24] basis set to perform geometry relaxation.

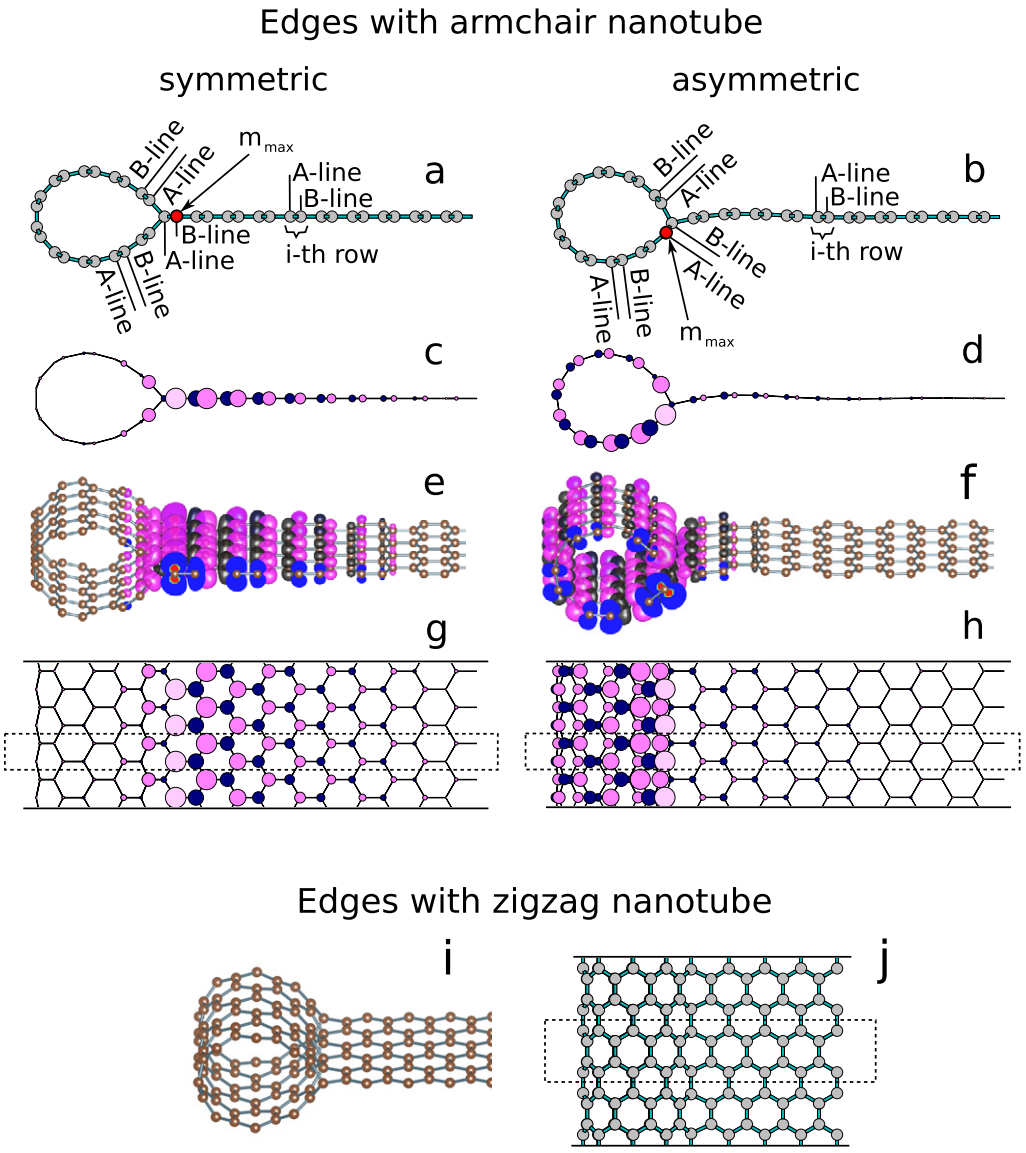

Figure 1. (a)–(h) Structure and spin density for symmetric (left) and asymmetric (right) AC nanotube terminated edges. (a), (b) Atomic structure; (c), (d) side, (e), (f) three-dimensional (3D) and (g), (h) top view of schematic spin representation. The box with a dashed line in (g), (h) indicates half of the unit cell in the density functional theory (DFT) calculation. For the symmetric case, the contribution to the magnetic moment from atoms belonging to the A- and B-sublattices are $m_{\mathrm{A}} = 0.958\mu_{\mathrm{B}}$ and $m_{\mathrm{B}} = -0.217\mu_{\mathrm{B}}$ (per half unit cell), and for the asymmetric case $m_{\mathrm{A}} = 1.048\mu_{\mathrm{B}}$ and $m_{\mathrm{B}} = -0.300\mu_{\mathrm{B}}$. The maximum of the magnetic moment is located on the atom indicated by the arrow with the value $m_{\mathrm{max}} = 0.379\mu_{\mathrm{B}}$ in both the symmetric and asymmetric cases. (i), (j) 3D and top view of AC nanoribbons terminated by ZZ nanotubes. The box with a dashed line in (j) indicates half of the unit cell in the DFT calculation.

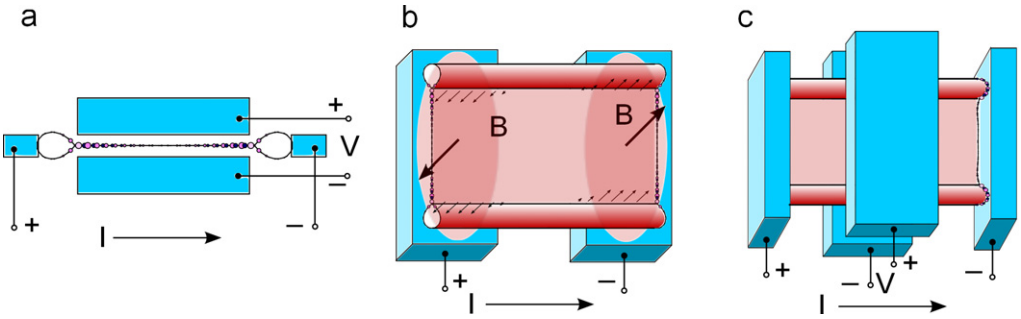

Figure 2. Sketch of spintronics devices based on carbon nanoribbons terminated by AC nanotubes. (a) A spin valve based on the symmetric case: a gate can be used to switch from the antiferromagnetically coupled state to the ferromagnetically coupled excited state, favoring spin transport from one nanotube to the other across the ribbon. (b) For both symmetric and asymmetric cases, high magnetoresistance could be achieved by applying magnetic fields of different sign at the ends of the nanoribbons, as proposed in [19] for ZZ nanoribbons. (c) For the asymmetric case, a gate along the ribbon could be used to switch between two half-metallic energy regions to realize either a spin filter or a spin valve.

In figure 4, we show the non-spin-polarized band structure and DOS of both symmetric and asymmetric ZZ nanoribbons with AC nanotubes at the edges. We see that indeed sharp peaks at the Fermi energy in the DOS are present as a consequence of the flat band located at this energy. This flat band resembles the one due to dangling bonds in ZZ nanoribbons. In [3], it was shown that the 57 reconstruction of the ZZ edges could split this band and shift it away from the Fermi energy. The termination with nanotubes leaves a band at the Fermi energy if no spin polarization is allowed. For the symmetric case, it is easy to visualize the character of this band as a p_z state decaying from the junction both in the nanoribbon and in the nanotube, as shown in figure 4(e). Instead of a change of bond character as for the 57 reconstruction, for our system it is the magnetic polarization that removes this state from the Fermi energy. In figure 5, we show the spin-polarized band structure and DOS, showing the splitting of the flat band at E_F into spin up and spin down levels and the consequent disappearance of the peaks at the Fermi energy in the DOS. We found that, in both the symmetric and asymmetric cases, there is spin polarization near the ribbon–tube junction, i.e. near the sp^3 hybridized carbon atoms. Note that the bond distance of these four-fold coordinated atoms is 1.52 Å like in diamond. The spin polarization is mainly located in the nanoribbon for the symmetric case and within the tube for the asymmetric case (see the isosurface plot of the spin density together with its symbolic representation in figures 1(c)–(h)). The up/down spins are distributed over the A/B sublattices, respectively. The label m_{max} indicates the atom with the highest magnetic moment. A possible explanation for the localization of the spin polarization can be found by realizing that the largest polarization is on the sp^2 atoms at the junction in between two sp^3 atoms (see red atoms in figure 3). The atoms with this particular configuration are either inside the nanotube or inside the nanoribbon and this corresponds to the location of the spin polarization. We are also tempted to conjecture that the localization results from a frustration mechanism. In fact in the symmetric case, where the polarization is located in the nanoribbon, the sp^3 atoms break the

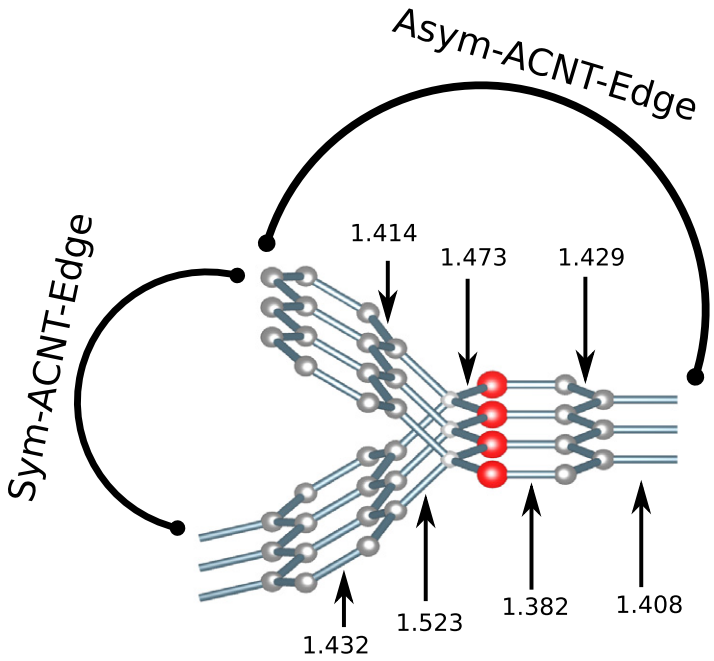

Figure 3. Sketch of the junction between the carbon nanoribbon and the AC nanotube. The junction itself is similar for both symmetric and asymmetric AC nanotube terminated edges, and the main difference is the different connection of the AC nanotube. The carbon–carbon distance indicated in the figure is for the symmetric case ($N = 5$ and $P = 20$), and the difference to the asymmetric case is negligible. In both the symmetric and asymmetric cases, the maximum magnetization is located at the sp^2 atoms (red) which are coupled to two sp^3 atoms (light gray).

bipartite symmetry in the ribbon (making magnetization possible) whereas for the asymmetric case, the sp^3 atom breaks the bipartite symmetry in the nanotube.

For the symmetric case, the value of the spin polarization increases with increasing nanoribbon width, and saturates at $1.50\mu_B$ per unit cell when the nanoribbon width is wider than 16 ZZ rows; for the asymmetric case, the spin polarization is always $1.50\mu_B$ per unit cell, irrespective of the nanoribbon width and nanotube radius (see table 1).

For the asymmetric case, the spins are located inside the two nanotubes and therefore the exchange interaction between opposite edges is negligible. For the symmetric case, the spins on the two edges are coupled antiferromagnetically, similarly to hydrogen terminated graphene edges [25, 26]: for the structure shown in figure 1(a), the energy of antiparallel spin configurations (see figure 1(g)) is 22 meV per unit cell lower than for parallel configurations. This sizeable coupling across the ribbon makes the symmetric systems promising as spin valve devices [27]. In figure 2(a), we show a configuration similar to that proposed for dumbbell graphene structures on the basis of the Hubbard Hamiltonian in the mean field approximation [28]. A gate could be used to bring the system from the antiferromagnetically coupled state to the ferromagnetically coupled excited state, favoring spin transport from one nanotube to the other across the ribbon. Moreover, for both the symmetric and asymmetric cases, the magnetic moments along the ribbon–tube junction are qualitatively

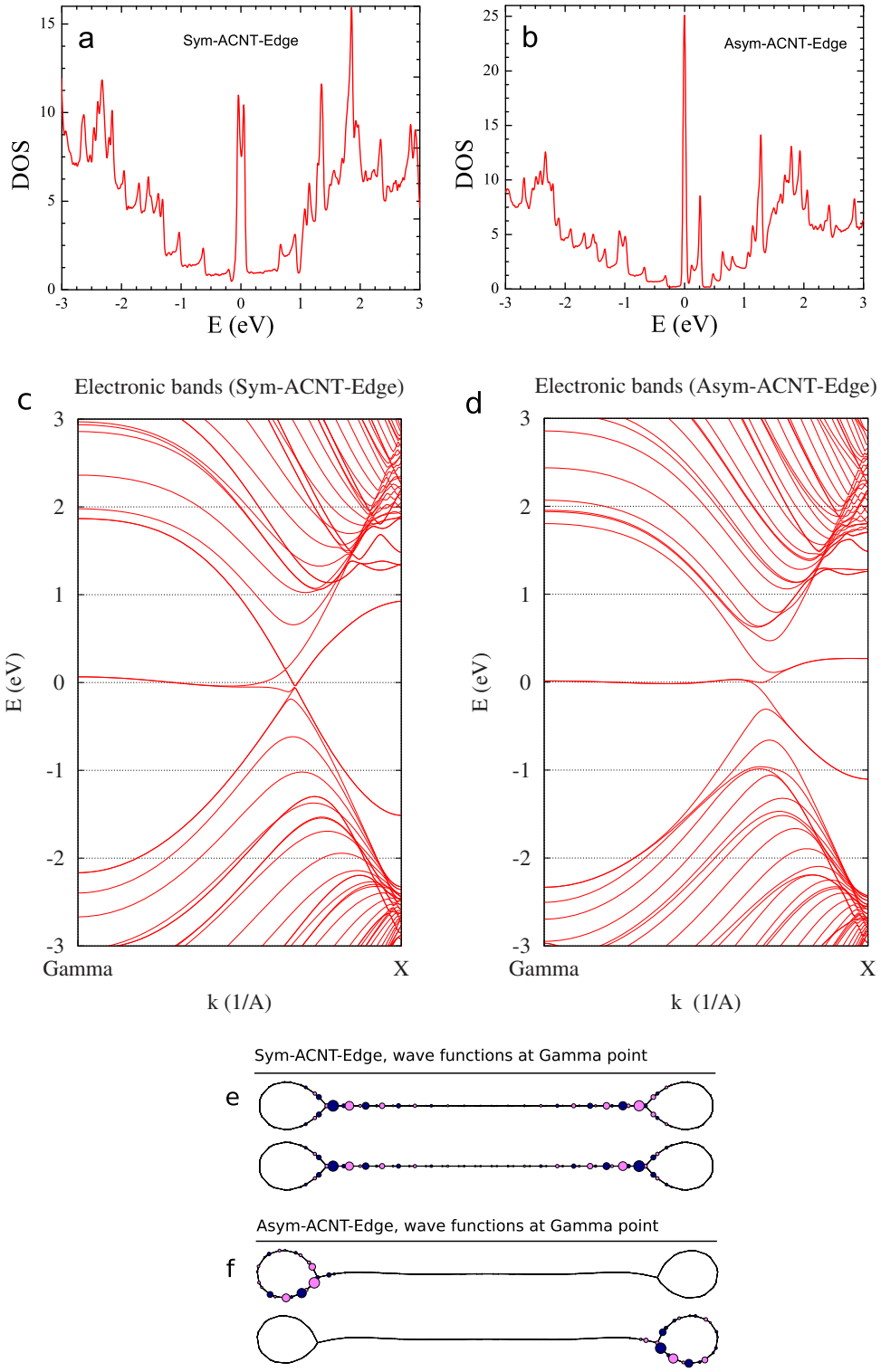

Figure 4. Non-spin-polarized DOS and band structure calculated by DFT for ZZ nanoribbons with (a), (c) symmetric and (b), (d) asymmetric AC nanotube terminated edges ($N = 5$ and $P = 20$ for both cases). The density of wave functions at Γ point are shown (e) for the symmetric case and (f) for the asymmetric case.

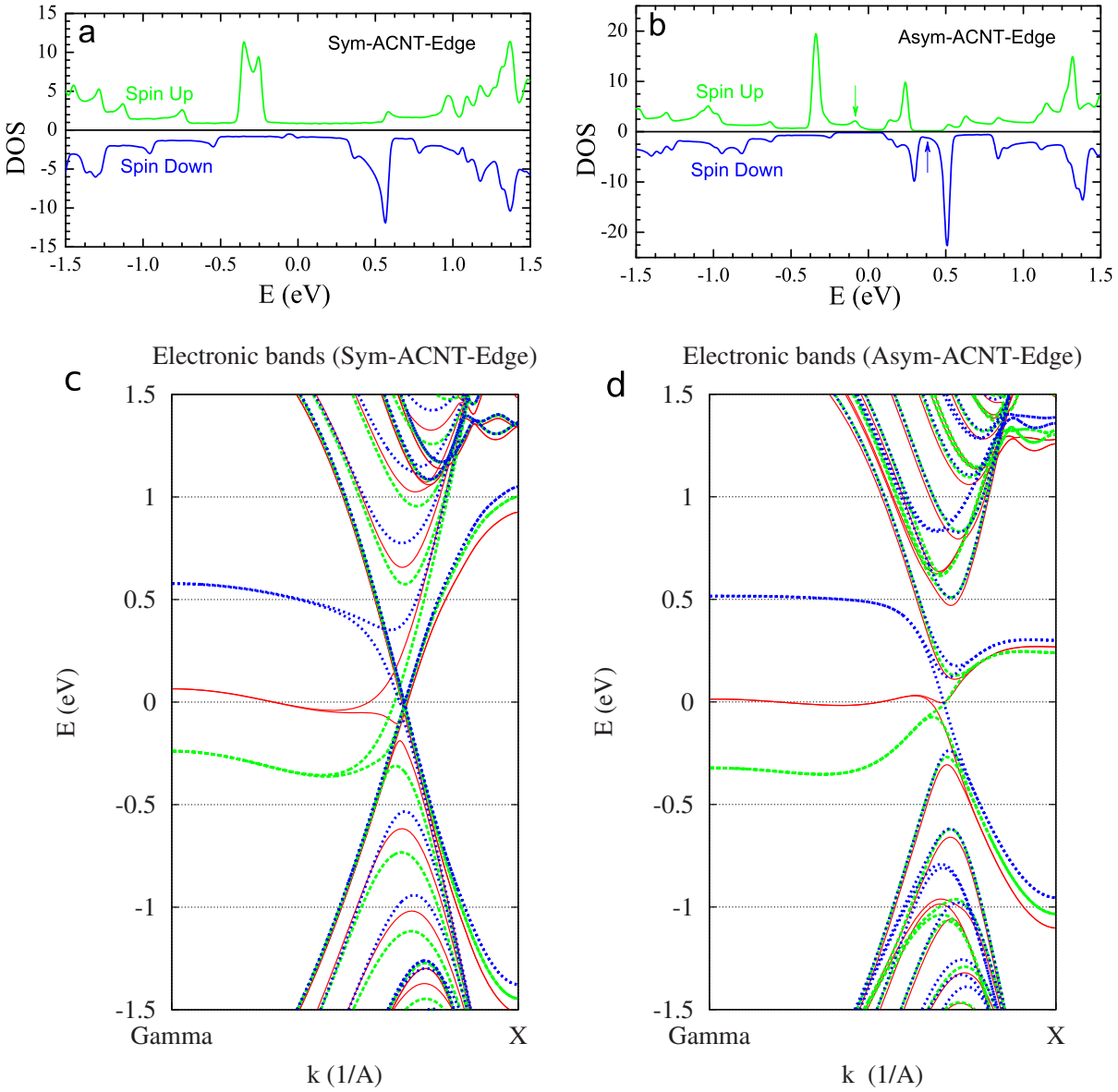

Figure 5. Spin-polarized DOS and band structure (bold dashed curves) calculated by DFT for ZZ nanorribons with (a), (c) symmetric and (b), (d) asymmetric AC nanotube terminated edges ($N = 5$ and $P = 20$ for both cases). The arrows in (b) indicate the half-metallic energy regions for either spin up or spin down. For comparison, the non-spin-polarized band structure is shown by red solid curves in (c), (d).

similar to the case of ZZ edges of nanoribbons. Therefore, high magnetoresistance could be expected, as proposed in [19] for nanoribbons with ZZ edges, by applying magnetic fields of different sign at the ends of the nanoribbon. A sketch of this device for our systems is shown in figure 2(b).

The spin-polarized DOS reveals other features of interest for spintronics related to half-metallic character. In figures 5(a) and (b), we show the spin-polarized DOS for both the symmetric and asymmetric cases, respectively. We see that the symmetric case is metallic for

Table 1. Total spin magnetization S (in units of μ_B per unit cell) as a function of the index of the AC nanotube (N, N) and the size of the nanoribbon P (in units of ZZ rows). The results in this table are for samples obtained by rolling the edges of the same unrolled graphene ribbon with a width of 40 ZZ rows.

N	P	S (symmetric)	S (asymmetric)
9	4	0.000	1.499
8	8	0.995	1.499
7	12	1.371	1.499
6	16	1.481	1.499
5	20	1.500	1.500
4	24	1.500	1.500
3	28	1.494	1.500

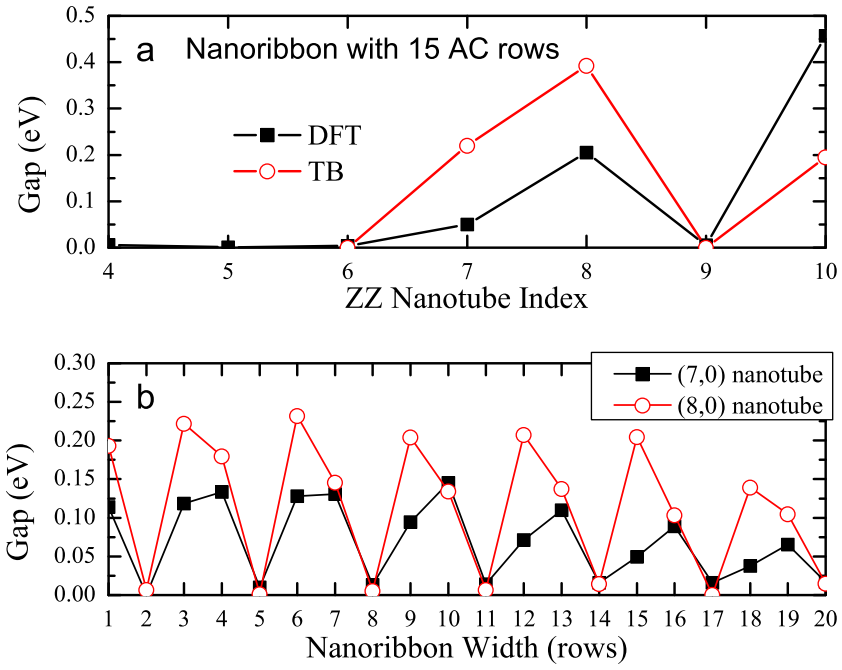

Figure 6. Band gap size-dependence in ZZ nanotube terminated AC nanoribbons. (a) Fixed nanoribbon with 15 AC rows for varying size of the terminating ZZ nanotube. (b) Fixed ZZ nanotube (8, 0 and 7, 0) edges for varying width of the AC nanoribbon.

both spins in the whole range of energy. The asymmetric case, instead, is a half-metal near the Fermi energy E_F; namely it is metallic for spin up and insulating for spin down. The half-metallic character of our systems provides opportunities as spin filters without the need of external electric fields [29], magnetic fields [30], ferromagnetic strips [31], impurities [32–34] or defects [35, 36]. Furthermore, there is the opposite half-metallic character at higher energies. Around 0.4 eV, there is insulating character for spin up and metallic character for spin down. As sketched in figure 2(c), a gate along the ribbon could be used to switch between these two half-metallic energy regions and affect selectively the spin transport.

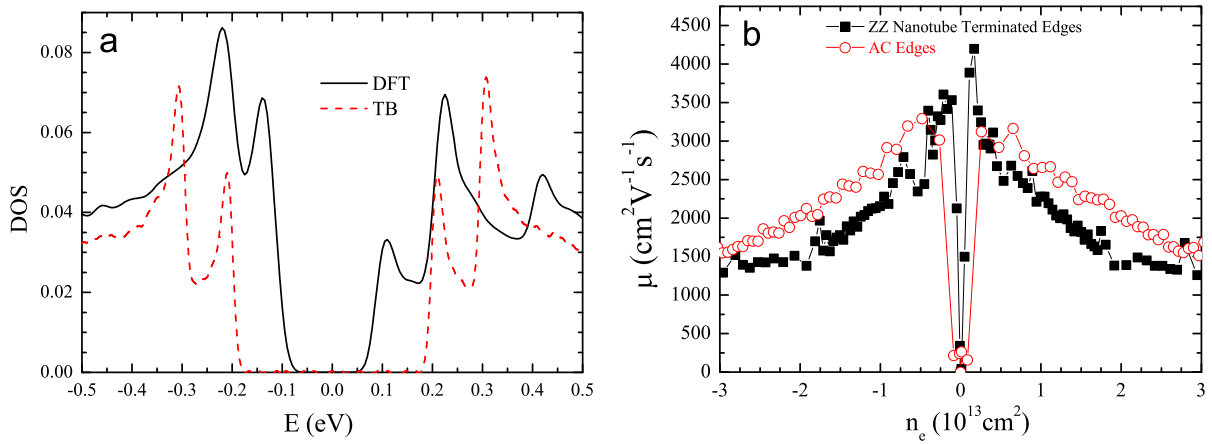

Figure 7. (a) Comparison of DOS of a nanoribbon with 15 AC rows terminated by (8,0) ZZ nanotubes calculated by DFT and TB. (b) Comparison of the mobility of a nanoribbon with 15 AC rows, terminated either by (8,0) ZZ nanotubes or by AC edges in TB. The charge density n_e is obtained from the density of state ρ in panel (a) by $n_e(E) = \int_0^E \rho(\epsilon)\,d\epsilon$. The sample contains $600\,000 \times 47$ carbon atoms for the case with ZZ nanotube terminated edges and $2000\,000 \times 15$ for the case with AC edges.

3. Edges terminated by zigzag nanotubes

We come now to the case of ZZ nanotubes shown in figures 1(i) and (j). For this case, there is only one type of ribbon–tube junction that preserves sublattice symmetry, implying that there is no magnetization or midgap states [8, 12]. The electronic structure and transport properties, however, strongly depend on the AC ribbon width and on the ZZ tube radius. In TB models, an AC nanoribbon is metallic if the number of AC rows is equal to $3l+2$, where l is a positive integer, and semiconducting otherwise [1, 37]. Furthermore, ZZ nanotubes are metallic for index equal to $3l$ [38]. In more general models, the properties of AC nanoribbons and ZZ nanotubes may differ from the ones predicted by TB, due to possible self-passivation of the edges for nanoribbons and for the σ–π band mixing for small nanotubes [38]. By using DFT calculations, we found that our joined system becomes a semiconductor with a gap of the order of a few hundreds of meV if both the nanoribbon and the nanotube are semiconducting. The energy gap as a function of geometry is shown in figure 6. The size of the nanotube has to be large enough for the opening of a band gap (figure 6(a)). For the joined system with semiconducting ZZ nanotubes, there is a clear periodicity (three ZZ rows) in the dependence of the energy gap on the nanoribbon width (figure 6(b)). For the studied cases, the value of the gap varies between 30 and 600 meV.

Since we want to calculate the transport properties by means of a simpler model, suitable for large samples, we have also calculated the energy structure of our system by π-band TB calculations where we consider only the nearest-neighbor hopping $t = 2.7$ eV between the carbon atoms [39, 40] for all bonds. The comparison between the gaps calculated by TB and DFT shown in figure 6(a) gives the same periodicity and qualitative agreement. For the case of an AC nanoribbon, with 15 rows terminated by (8, 0) ZZ nanotubes, we compare in figure 7(a)

the TB and DFT DOS, which again are in qualitative agreement thus supporting the validity of the transport calculations we show next. The electronic transport properties of a semiconducting nanoribbon with or without nanotube terminated edges are obtained by using large-scale TB simulations with about 30 million carbon atoms [39, 40]. In figure 7(b), we show that the electronic mobility parallel to the edges as a function of charge density is quite similar in these two cases. The mobility of the joined system is about 2250 $cm^2\ V^{-1}\ s^{-1}$ at charge density $n_e \sim 10^{13}\ cm^2$, which is only slightly smaller than that of the AC nanoribbon at the same charge concentration.

4. Summary and conclusion

In summary, we have studied the electronic and magnetic properties of graphene nanoribbons with three types of nanotube terminated edges. The spin magnetization is found to be $1.5\mu_B$ per unit cell in the ground state of both symmetric and asymmetric AC nanotube terminated edges. For symmetric AC nanotube terminated edges, the spin density is located in the ribbon whereas, for the asymmetric case, it is located within the tube. In the ZZ nanotube terminated edges, there is a band gap opening of the order of a few hundreds of meV if the constituent tube and nanoribbon are both semiconducting. The conductivity and mobility in the presence of ZZ nanotube terminated edges are comparable to those of the AC nanoribbon itself.

Our calculations suggest that these systems are not only advantageous because the edges are protected against any kind of chemically induced disorder but also because, by tailoring the ribbon/tube structure, they offer a wealth of possible applications for transport and spintronics.

Acknowledgments

The support from the Stichting Fundamenteel Onderzoek der Materie (FOM) and the Netherlands National Computing Facilities foundation (NCF) is acknowledged. We acknowledge support from the EU-India FP-7 collaboration under MONAMI and the grant CONSOLIDER CSD2007-00010.

References

[1] Son Y W, Cohen M L and Louie S G 2006 *Phys. Rev. Lett.* **97** 216803
[2] Han M Y, Özyilmaz B, Zhang Y and Kim P 2007 *Phys. Rev. Lett.* **98** 206805
[3] Koskinen P, Malola S and Häkkinen H 2008 *Phys. Rev. Lett.* **101** 115502
[4] Wassmann T, Seitsonen A P, Saitta A M, Lazzeri M and Mauri F 2008 *Phys. Rev. Lett.* **101** 096402
[5] Girit C O *et al* 2009 *Science* **323** 1705–8
[6] Liu Z, Suenaga K, Harris P J F and Iijima S 2009 *Phys. Rev. Lett.* **102** 015501
[7] Wimmer M, Akhmerov A R and Guinea F 2010 *Phys. Rev.* B **82** 045409
[8] Yazyev O V 2010 *Rep. Prog. Phys.* **73** 056501
[9] van Ostaay J A M, Akhmerov A R, Beenakker C W J and Wimmer M 2011 *Phys. Rev.* B **84** 195434
[10] Jia X, Campos-Delgado J, Terrones M, Meunier V and Dresselhaus M S 2011 *Nanoscale* **3** 86–95
[11] Kunstmann J, Özdoğan C, Quandt A and Fehske H 2011 *Phys. Rev.* B **83** 045414
[12] Katsnelson M I 2012 *Graphene: Carbon in Two Dimensions* (Cambridge: Cambridge University Press)
[13] Koskinen P, Malola S and Häkkinen H 2009 *Phys. Rev.* B **80** 073401
[14] Chuvilin A, Meyer J C, Algara-Siller G and Kaiser U 2009 *New J. Phys.* **11** 083019

[15] Kroes J M H, Akhukov M A, Los J H, Pineau N and Fasolino A 2011 *Phys. Rev.* B **83**
[16] Ivanovskaya V V, Zobelli A, Wagner P, Heggie M I, Briddon P R, Rayson M J and Ewels C P 2011 *Phys. Rev. Lett.* **107** 065502
[17] Chernozatonskii L A, Sheka E F and Artyukh A A 2009 *JETP Lett.* **89** 352–6
[18] Artyukh A A, Chernozatonskii L A and Sorokin P B 2010 *Phys. Status Solidi* b **247** 2927–30
[19] Kim W Y and Kim K S 2008 *Nature Nanotechnol.* **3** 408–12
[20] Soler J M, Artacho E, Gale J D, Garcia A, Junquera J, Ordejon P and Sanchez-Portal D 2002 *J. Phys.: Condens. Matter* **14** 2745–79
[21] Sanchez-Portal D, Ordejon P and Canadell E 2004 *Principles and Applications of Density Functional Theory in Inorganic Chemistry II* (Berlin: Springer) p 113
[22] Artacho E *et al* 2008 *J. Phys.: Condens. Matter* **20** 064208
[23] Perdew J P, Burke K and Ernzerhof M 1996 *Phys. Rev. Lett.* **77** 3865
[24] Junquera J, Paz O, Sánchez-Portal D and Artacho E 2011 *Phys. Rev.* B **64** 235111
[25] Yazyev O V and Katsnelson M I 2008 *Phys. Rev. Lett.* **100** 047209
[26] Bhandary S, Eriksson O, Sanyal B and Katsnelson M I 2010 *Phys. Rev.* B **82** 165405
[27] Hill E W, Geim A K, Novoselov K, Schedin F and Blake P 2006 *IEEE Trans. Magn.* **42** 2694–6
[28] Ma Z and Sheng W 2011 *Appl. Phys. Lett.* **99** 083101
[29] Son Y W, Cohen M L and Louie S G 2006 *Nature* **444** 347–9
[30] Abanin D A, Lee P A and Levitov L S 2006 *Phys. Rev. Lett.* **96** 176803
[31] Zhang Y T, Jiang H, Sun Q F and Xie X C 2010 *Phys. Rev.* B **81** 165404
[32] Hod O, Barone V, Peralta J E and Scuseria G E 2007 *Nano Lett.* **7** 2295–9
[33] Zheng X H, Wang R N, Song L L, Dai Z X, Wang X L and Zeng Z 2009 *Appl. Phys. Lett.* **95**
[34] Soriano D, Muñoz Rojas F, Fernández-Rossier J and Palacios J J 2010 *Phys. Rev.* B **81** 165409
[35] Martins T B, da Silva A J R, Miwa R H and Fazzio A 2008 *Nano Lett.* **8** 2293–8
[36] Lisenkov S, Andriotis A N and Menon M 2012 *Phys. Rev. Lett.* **108** 187208
[37] Ezawa M 2006 *Phys. Rev.* B **73** 045432
[38] Dubois S M M, Zanolli Z, Declerck X and Charlier J C 2009 *Eur. Phys. J.* B **72** 1
[39] Wehling T O, Yuan S, Lichtenstein A I, Geim A K and Katsnelson M I 2010 *Phys. Rev. Lett.* **105** 056802
[40] Yuan S, De Raedt H and Katsnelson M I 2010 *Phys. Rev.* B **82** 115448